Astron. Astrophys. 290, 609–622 (1994)

ASTRONOMY AND ASTROPHYSICS

Near-IR excess of Be stars*,**

S.M. Dougherty[1], L.B.F.M. Waters[2,3], G. Burki[4], J. Coté[3], N. Cramer[4], M.H. van Kerkwijk[5], and A.R. Taylor[6]

[1] Chemical and Physical Sciences, John Moores University of Liverpool, Byrom Street, Liverpool, L3 3AF, UK
[2] Astronomical Institute "Anton Pannekoek", University of Amsterdam, Kruislaan 403, NL-1098 SJ Amsterdam, The Netherlands
[3] SRON Laboratory for Space Research, P.O. Box 800, NL-9700 AV Groningen, The Netherlands
[4] Observatoire de Genève, CH-1290 Sauverny, Switzerland
[5] California Institute of Technology, California, CA 91125, USA
[6] Department of Physics and Astronomy, University of Calgary, 2500 University Dr. N.W., Calgary, AB, Canada

Received 22 October 1993 / Accepted 13 April 1994

Abstract. The near-IR excess emission of 144 Be stars is derived from visual and near-IR observations. The quasi-simultaneous nature of the observations provide colour excesses that are independent of temporal variations. Colour-colour diagrams are used to identify stars with excess colours markedly different from the bulk of the sample stars. The near-IR emission of four stars that have markedly different colours is attributed to the presence of a binary companion or thermal dust emission. The percentage of stars with a significant excess increases with wavelength. The excess emission increases with wavelength and the largest excesses occur in stars of earlier spectral type. The near-IR excess colours are examined and compared to theoretical excess colours calculated from a simple bremsstrahlung emitting disc model with a radial density distribution of the form $\rho \propto r^{-\beta}$. The effect of model parameters on the excess colours is discussed. The observed excesses for the bulk of the stars are well fit by circumstellar discs with radii greater than $\sim 10R_*$ and with a density index β, in the range $2.0 - 5.0$. This is very similar to the range of values previously determined by Waters et al. (1987) from *IRAS* far-IR observations. A small number of stars cannot be reconciled with discs with a constant density index out to $10R_*$. It is argued that the circumstellar plasma around these stars has a change in structure at $\sim 2 - 10R_*$. The possibilities of disc truncation or a change in the density index as the cause of the structure change are discussed.

1. Introduction

The first detection of an excess of near-IR emission from Be stars compared to that from normal stars of the same spectral types was that by Johnson et al. (1966). Johnson (1967) concluded that, in a sample of 85 early-type stars, all the Be stars had an excess $(K - L)$ colour. He attributed this to IR emission from circumstellar material. Woolf et al. (1970) suggested from observations out to 10 μm that the IR excess of Be stars may be due to free-free emission from the same ionised circumstellar material that gives rise to the Hydrogen Balmer emission lines, a characteristic spectral feature of all Be stars. Woolf et al. could not rule out the possibility of the excess being due to thermal dust emission from their observations alone. Allen (1973) reached the same conclusion from near-IR observations of a large sample of Be stars.

By observing Be stars at wavelengths as long as 20 μm, Gehrz et al. (1974) demonstrated that the near-IR excess emission in Be stars is due to free-free emission. From observations of 33 Be stars, they concluded that circumstellar dust could not produce the observed near-IR energy distribution. By assuming that the excess emission became optically thick at some wavelength ≤ 20 μm, Gehrz et al. were able to deduce characteristic densities $\sim 7 \times 10^{-13}$ g cm^{-3} and radii $\sim 4R_*$ for the near-IR emitting plasma envelope. Subsequent observations at millimeter (Waters et al. 1989, 1991) and radio wavelengths (Taylor et al. 1990; Dougherty & Taylor 1992) indicate that the high density ionised gas can extend to very large distances from the star (up to $\sim 2000R_\odot$).

The high density circumstellar plasma gives rise to strong emission lines, particularly those of the Hydrogen Balmer series. The shape and strength of these lines suggest that the high density plasma has a low outflow velocity (~ 10 km s^{-1}). However, observations of UV resonance lines of highly ionised species e.g. Si IV, C V, indicate high velocity (~ 1000 km s^{-1}), low density plasma. These apparently conflicting observations are commonly interpreted as arising from a circumstellar envelope that has an equatorially enhanced density distribution. In this model, the excess continuum emission and optical line emission originate in a region of high density, low velocity plasma in the equatorial plane of the star, and the UV resonance lines arise in low density, high velocity material at higher stellar latitudes.

Send offprint requests to: S.M. Dougherty

* Partly based on observations obtained at ESO, La Silla, Chile

** Table 1 is only available in electronic form: see editorial in A&A 1992, Vol. 266 No. 2, page E1

This model has been very successful in explaining quantitatively many observations of Be stars. Most notably, the circumstellar plasma around the Be-shell star ψ Persei has been resolved at radio wavelengths and clearly shows that the high density plasma has a non-spherically symmetric distribution (Dougherty & Taylor 1992). In addition, linear polarisation observations of Be stars require electron scattering of photospheric emission by free electrons that have a non-spherically symmetric distribution (Poeckert & Marlborough 1976; McLean & Brown 1978; Poeckert et al. 1979).

The continuum spectrum of the circumstellar gas can be used to place constraints on the structure of the high density gas. In particular, the slope of the spectra is strongly dependent on the radial density distribution of the emitting gas (e.g. see Olnon 1975; Wright & Barlow 1975). *IRAS* observations of Be stars indicate that the far-IR continuum arises from gas with a radial power law distribution of the form $\rho \propto r^{-\beta}$ out to $\sim 30 - 60 R_{\odot}$ (Waters 1986b). However, this simple power-law behaviour does not appear to extend to large distances from the underlying star. Comparison of the slope of the spectrum between the far-IR and millimeter wavelength regions and the slope at radio wavelengths show a turndown in the far-IR–millimeter wavelength region of the spectrum of several Be stars (Waters et al.1991). Upper limits to the millimetre emission in other Be stars suggest a turndown a shorter wavelengths. This indicates a change in the density gradient of the outer regions of the circumstellar envelope. The cause of the change in the density gradient is presently unknown.

To investigate the structure of the high density circumstellar envelopes of Be stars at near-IR wavelengths, we have obtained quasi-simultaneous visual and near-IR observations of a large number of stars as part of an observing campaign of B and Be type stars in conjunction with the *ROSAT* X-ray all-sky survey. In this paper we present the analysis of the near-IR excess emission of Be stars. The quasi-simultaneous nature of the observations provide excess values that are independent of temporal continuum variations on time scales greater than a few weeks, variations that have restricted previous studies of the IR excess of large samples of Be stars e.g. Waters et al.1987, Dougherty et al.1991. A simple bremsstrahlung emitting disc model is used to interpret the excess colours. In Sect. 3.2 we describe the colour-colour relationships of the stars. The theoretical colours as a function of the disc model parameters are discussed in Sect. 4 and the results of these calculations are compared with the observed excess colour-colour relationship of the sample stars. Section 5 summarises the results.

2. Observations

The programme stars were selected from the Be stars in the Bright Star Catalogue (hereafter BSC; Hoffleit & Jaschek 1982) and the BSC Supplement (Hoffleit et al.1983). Observations at visual and near-IR wavelengths were obtained for a large number of Be stars from both northern and southern hemisphere observatories (Dougherty et al.1991a; Dougherty 1993a; Burki et al., in preparation). There are a few stars for which only observations at either visual or near-IR wavelengths were obtained. To complete the data set, observations at the "missing" wavelength region were taken from the literature. Visual observations of 29 stars were taken from the Geneva photometric catalogue (Rufener 1988) and near-IR observations for 14 stars from Dachs et al. (1988).

In total, we have collected observations for 144 Be stars. The typical uncertainty in the visual observations is a few millimagnitudes. and in the near-IR observations are $0\overset{m}{.}03 - 0\overset{m}{.}05$ at the J, H and K bands respectively and $0\overset{m}{.}06$ at L band.

3. IR excess of Be stars

3.1. Interstellar reddening

The first step in calculating the IR excess emission is to account for the effects of interstellar reddening. The most common method of determining the effects of interstellar reddening is estimation of the excess $[B-V]$ colour, $E[B-V]$ from the intrinsic $[B-V]_o$ colour of the star i.e.

$$E[B-V] = [B-V] - [B-V]_o = E[B-V]_{is},$$

where $E[B-V]_{is}$ is the reddening due to interstellar material along the line of sight to the star. Early-type Be stars (B0–B2) are known to have an excess of emission in the Paschen continuum due to free-free and bound-free processes in circumstellar material (Schild 1978, 1983). The excess $[B-V]$ colour is then given by

$$E[B-V] = [B-V] - [B-V]_o = E[B-V]_{is} + E[B-V]_{cs},$$

where $E[B-V]_{cs}$ is the reddening due to the presence of circumstellar material. Obviously, for stars with an excess of emission in the Paschen continuum, $E[B-V]$ is overestimated due to the presence of circumstellar material. For example, an $E[B-V]_{cs}$ of $0\overset{m}{.}1$ leads to a de-reddened V magnitude that is $\sim 0\overset{m}{.}3$ too bright i.e. the derived V band flux is overestimated. However, the effect of the interstellar reddening correction on the IR colours, on which the analysis in this study is based, is smaller than the uncertainty. If $E[B-V]$ is overestimated by $0\overset{m}{.}1$, the near-IR colour $[J-H]$ will be too blue by $0\overset{m}{.}03$, compared to the estimated uncertainty in the colour of $0\overset{m}{.}06$.

There are other techniques for estimating $E[B-V]_{is}$ that are independent of the presence of circumstellar material e.g. using the interstellar absorption feature at 2175Å (Beeckmans & Hubert-Delplace 1980), and main sequence field stars (Goraya 1984). Unfortunately, these methods have only been applied to a small number of Be stars in our sample. Making our observations with the Geneva photometric system allowed the possibility of using the interstellar reddening-free parameters, X and Y, to estimate the intrinsic $[B-V]_o$ colours of each of our sample stars (Cramer & Maeder 1979; Cramer 1982; North & Nicolet 1990). However, in the presence of circumstellar emission, the Geneva X and Y parameters can lead to intrinsic colours that are too blue. Hence, the excess $[B-V]$ colours are overestimated.

In this study we use the MK spectral classification to establish the excess colour. Values of the intrinsic $[B-V]_o$ were taken

from Cramer (1982). As a comparison, values of $E[B-V]$ obtained from spectral types are compared with those obtained using the 2175Å absorption feature (see Table 1 (only available in electronic form)).

3.2. Colour-colour diagrams

Before calculating IR excesses for the sample stars it is beneficial to examine the colour-colour diagrams of Be stars. From these diagrams it is possible to identify features of the IR emission common to the sample stars and to identify stars with anomalous colours.

The de-reddened observations are shown in the colour-colour diagrams of Figs. 1 and 2. Figure 1 shows the visual−IR colours as a function of $[B-V]_o$ and Fig. 2 is the near-IR colour-colour relationships. Also plotted are the colour-colour relationships for normal B-type stars, taken from Dougherty et al. (1993b).

Several groups of Be stars can be distinguished in the visual−IR colour-colour diagram: stars with colours closely the same as "normal" B-type stars; stars that have significantly redder colours than normal B-type stars; and a few stars with $[V-m_\lambda]$ colours bluer than expected for normal B-type stars.

The stars that have colours similar to the normal B-type star colour-colour relationship for a particular IR passband are those Be stars that have no detectable excess at that wavelength. There are many Be stars that have colours that are significantly redder than expected for the spectral type of the star. This indicates an excess of emission at those wavelengths. In general, the largest excesses occur for the earlier spectral type stars. Also, for a given spectral type, the excess, on average, increases with wavelength. These features have been noted before by several authors (e.g. Gehrz et al.1974; Dachs et al.1988; Coté & Waters 1987; Dougherty et al.1991a) and are interpreted as arising from optically thin or partially optically thick free-free and free-bound emission. Dust also gives an increasing excess with wavelength. However, the IR colours of dust emission are usually very different from those arising from bremsstrahlung processes, particularly at longer IR wavelengths. At far-IR wavelengths, Coté and Waters conclude that the circumstellar emission from most Be stars detected by *IRAS*, with the exception of 51 Oph, is due to free-free emission. 51 Oph is a Be star with circumstellar emission due to dust (Waters et al.1988a). In both Figs. 1 and 2, 51 Oph has a noticeably large excess for its spectral type and its IR colours are very red, particularly at longer wavelengths compared to other stars in the sample e.g. $[V-L] = 1\overset{\mathrm{m}}{.}32$ as compared to $-0\overset{\mathrm{m}}{.}19$ for a normal B9 star.

There are a number of other stars beside 51 Oph that have IR colours that are markedly different to the bulk of the sample stars. These colours are attributed to the presence of a binary companion star. Included in Fig. 2 is the approximate relationship for main sequence stars of spectral types A0 to K0 (Koornneef 1983a). For the companion star to affect the IR colours of the binary system it has to be sufficiently luminous at IR wavelengths to dominate the IR emission from the system. Furthermore, to be noticeable in the IR colour-colour diagram it has to have IR colours different to those of Be stars. This rules out the possibility of identifying Be stars with early-type companions using this method since early-type companions have similar colours to Be stars. However, as shown in Fig. 2, late-type companions have very red colours compared to the Be stars. The binary systems AX Mon (HD 45910) (B2eIII+K0III) and HR 2577 (B3eIV+K2II) are two such stars. The star HR 2545 has similar colours to AX Mon and HR 2577, suggesting that it is also a Be + late-type binary system. This star is a known wide binary, with a B9 companion but a late-type companion has not been previously noted in the literature. The stars β Mon and CX Dra also have IR colours that are different to the bulk of the sample. β Mon is a triple system, consisting of three Be stars. β Mon A is a spectroscopic binary (BSC), that may have a companion of spectral type later than B-type. Likewise, CX Dra is also identified in the BSC as a spectroscopic binary, the IR colours suggesting the presence of a late A or early F-type companion.

Since the properties of IR excess from Be stars as a group are of interest, neither the properties of the late-type binary systems nor 51 Oph which obviously have IR colour characteristics that are very different to the bulk of the Be stars in the sample, will be discussed further.

A small number of stars apparently have bluer $[V-m_\lambda]$ colours than expected for the photosphere of the star. This leads to a "negative" excess colour. The 3σ lines in Fig. 1 show that, for a few stars, the magnitude of the negative excess is significant and cannot be attributed to scatter in the data due to random noise. Three possible causes are considered: excess emission in the Paschen continuum, short time scale variability ($\sim$ a few weeks) at the visual and/or IR passbands, and attenuation of photospheric emission by cool circumstellar plasma. The stars that have the most negative excess (π Aqr, HR 8375 and 120 Tau) each have an excess $[B-V]$ colour greater than $0\overset{\mathrm{m}}{.}2$. If $E[B-V]$ is overestimated due to an excess in the Paschen continuum then the $[V-J]$ colour will appear to be bluer. In the case of π Aqr, $E[B-V] = 0.2$. If it is assumed for the moment that the interstellar reddening for this star is negligible i.e. the reddening is solely due to circumstellar material, then the $[V-J]$ colour would appear to be bluer by $\sim 0\overset{\mathrm{m}}{.}4$. Compensating for this would give π Aqr a $[V-J]$ colour similar to other Be stars at the same $[B-V]$ colour. However, even though this explanation can account for the blue colour of π Aqr compared to other Be stars, it cannot be a complete explanation since one would expect more of the early-type Be stars with $E[B-V] > 0\overset{\mathrm{m}}{.}2$ to have a negative excess.

Each of the stars that have a negative excess have been determined to be variable at near-IR wavelengths (Dougherty & Taylor 1994). Furthermore, these stars have extensive histories of variations in the optical (e.g. Slettebak 1982). This study is based on observations at visual and near-IR wavelength regions that were obtained, at most, a few months apart. This rules out variations on time scales of a few months or longer as the cause. Interestingly, none of the excesses derived using either the IR data of Dachs et al. (1988) (epoch 1983) or the visual data from Rufener (1988) are significantly negative. Thus, for variability

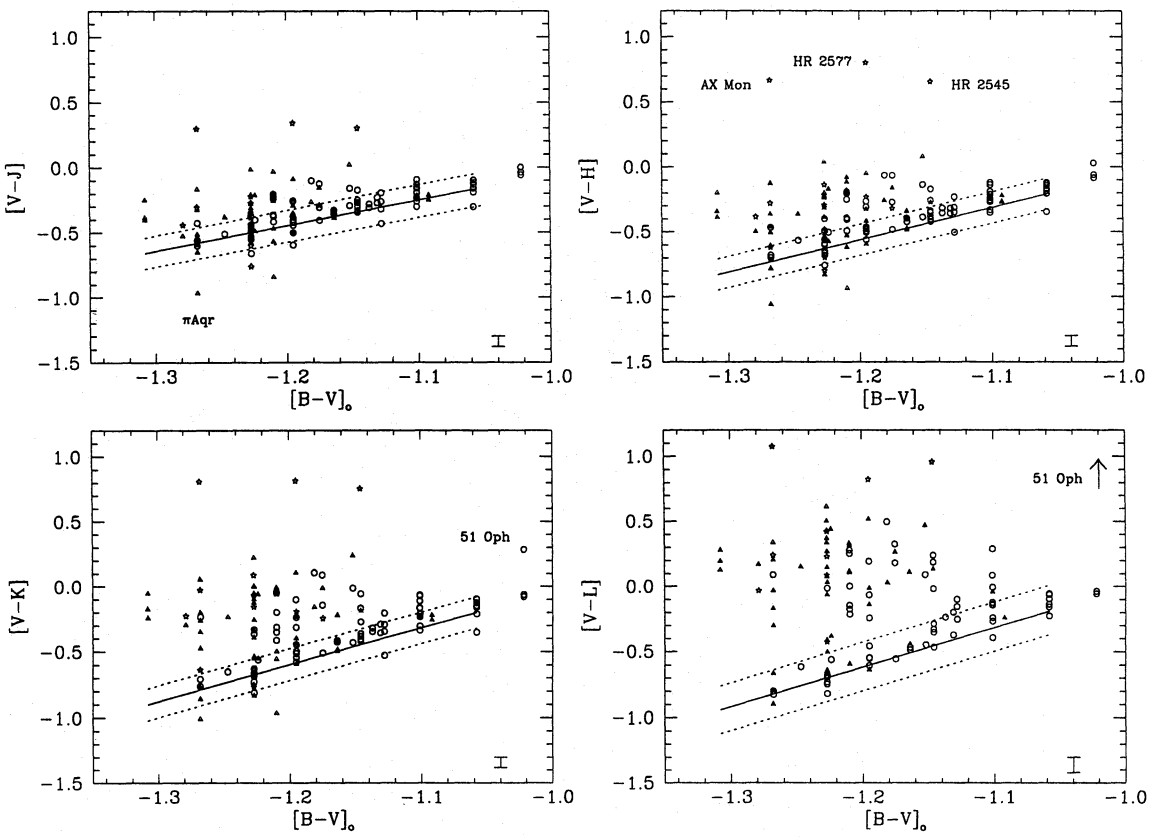

Fig. 1. Visual−IR colours of Be stars as a function of $[B-V]_o$. The solid lines represent the relationship for normal B-type stars between B0 and B9 (Dougherty et al.1993b). The dashed lines are the 3σ distance from the normal B star relationship. Different symbols represent different ranges of $E[B-V]$: open circles for $0-0.1$; solid triangles for $0.1-0.3$; and stars for $0.3-1.0$. The typical 2σ uncertainty in each point is given in the lower right-hand corner of the figures

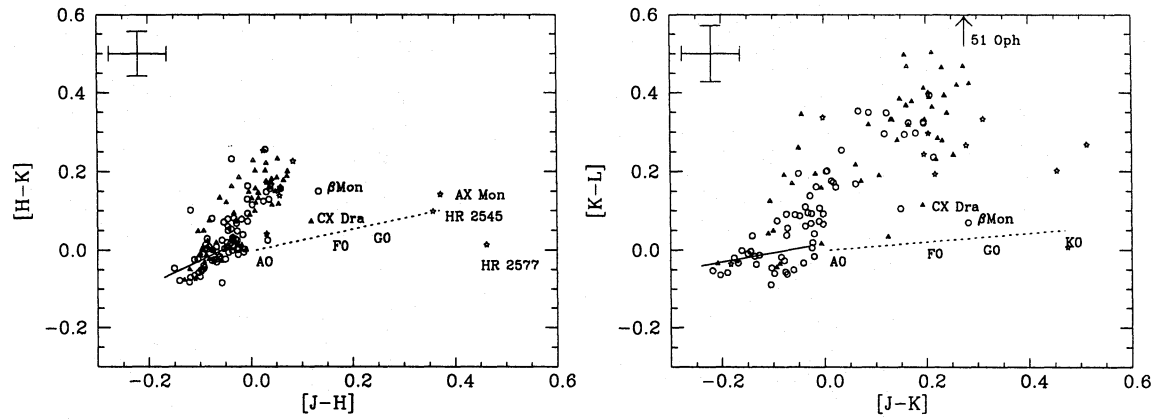

Fig. 2. Near-IR colour-colour diagram for Be stars. The solid lines represent the relationship for normal B-type stars between B0 and B9 (Dougherty et al.1993b). Different symbols represent different ranges of $E[B-V]$ as in Fig. 1. The typical 2σ uncertainty in the points is given in the upper left-hand corner of the figures. The dashed line is the approximate colour-colour relationship for main sequence stars of spectral types A0 to K0 (Koornneef 1983a)

to be the cause of negative excess, continuum variations of the order of a few tenths of a magnitude would have to happen on time scales shorter than a few months.

Another possible cause of negative excess is cool circumstellar plasma along the line of sight to the star. The photospheric near-IR emission will then be absorbed by the circumstellar material along the line of sight, the absorption being dependent on the density and temperature of the circumstellar material. If the material is sufficiently cool relative to the effective temperature of the underlying photosphere, absorption can give rise to a total emitted IR flux from the star and circumstellar envelope that is less than that expected from the photosphere alone. This mechanism is described in detail in Sect. 4.3.3.

3.3. IR excess emission

Under the assumption that the photospheric emission in Be stars arises from the photosphere of a normal B-type star, the visual−IR colour excess at wavelength λ is given by

$$CE[V - m_\lambda] = [V - m_\lambda] - [V - m_\lambda]_o,$$

where $[V - m_\lambda]_o$ is the intrinsic colour of the underlying B star and m_λ is the IR magnitude at each of the IR passbands and $[V - m_\lambda]$ is the observed visual−IR colour corrected for interstellar reddening.

To estimate the magnitude of the photospheric emission the $[V - m_\lambda]_o, [B - V]_o$ colour relationships as derived for normal B-type stars in the Geneva photometric system (Dougherty et al.1993b) were used. To determine $[V - m_\lambda]_o$ colours, values of $[B - V]_o$ were derived from spectral type, as given by Cramer (1982), to avoid overestimation of the intrinsic colours due to the presence of circumstellar material, as described earlier. The $CE[V - m_\lambda]$ colours are given in Table 1. The uncertainty in these excess colours is $\sim 0\overset{m}{.}05$ for colours with the J, H, K bands and $\sim 0\overset{m}{.}06$ at L band.

In this analysis it is tacitly assumed that there is no error in the spectral classification of the stars. Misclassification would have the greatest effect on B0−B3 and B8−B9 stars where the intrinsic colour differences per subclass are $0\overset{m}{.}04$ (Dougherty et al.1993b). A misclassification by one subclass in these spectral types would produce an excess visual−IR colour that is incorrect by $\sim 0\overset{m}{.}08$ at J band and $0\overset{m}{.}12$ at L. However, for IR excess colours these offsets reduce to $\sim 0\overset{m}{.}02$ for $CE[J-H]$ and $0\overset{m}{.}04$ for $CE[J - L]$. These offsets are similar in magnitude to the uncertainty in the observed magnitudes and are small compared to the absolute error in the excess IR colours.

In Table 2 the number of stars with a significant excess i.e. $CE[V - m_\lambda] > 3\sigma$, and the total number of stars at each passband are given. The percentage of stars with excess emission increases with wavelength, as expected from Fig. 1, with $\sim 50\%$ and 60% of the sample stars having significant excess emission at K and L bands respectively.

In Sect. 3.2 it was noted that the excess increases as a function of wavelength. Figure 3 shows the distribution of $CE[V - m_\lambda]$ for each IR passband. The mean of the distributions is also indicated. At J and H bands the bulk of the sample have no excess. However, at K and L bands, there is a larger number of stars with significant excess. The mean of the distributions increases with wavelength, indicating that for Be stars *as an ensemble*, the magnitude of the excess increases with wavelength. At L band a bi-modal distribution of Be stars is suggested: stars with an excess $> 0\overset{m}{.}4$ and stars with small excess. It is interesting that a similar bi-modal distribution is seen in excesses at far-IR wavelengths (Waters, private communication).

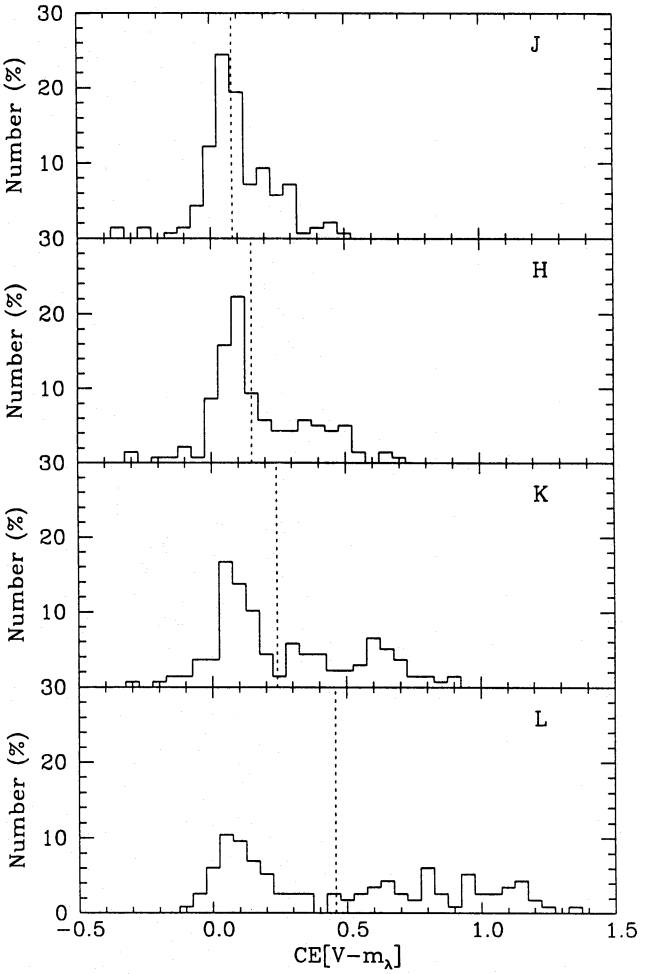

Fig. 3. The distribution of excess $[V - m_\lambda]$ colours. The late-type binaries and 51 Oph are not included. The vertical dashed lines are the means of the distributions: 0.08, 0.15, 0.24, 0.46 at J, H, K and L bands respectively

Table 2. Summary of the number of stars with excess $[V - m_\lambda]$ colour. The late-type binaries and 51 Oph are not included

m_λ	Total	$> 3\sigma$	%
J	139	43	31
H	139	57	41
K	138	70	51
L	115	71	62

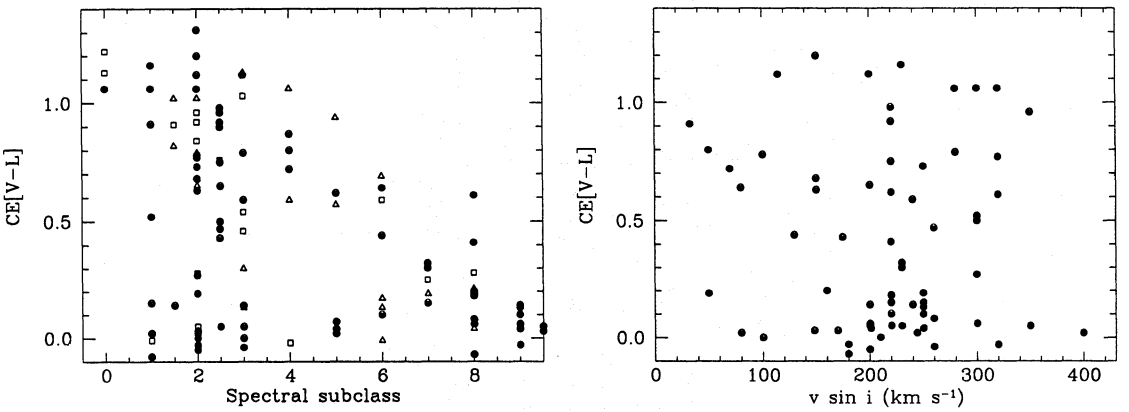

Fig. 4. a The excess $[V - L]$ colour as a function of spectral type. Luminosity classes are represented by □ (III), △ (IV) and • (V). **b** The excess $[V - L]$ colour as a function of $v \sin i$

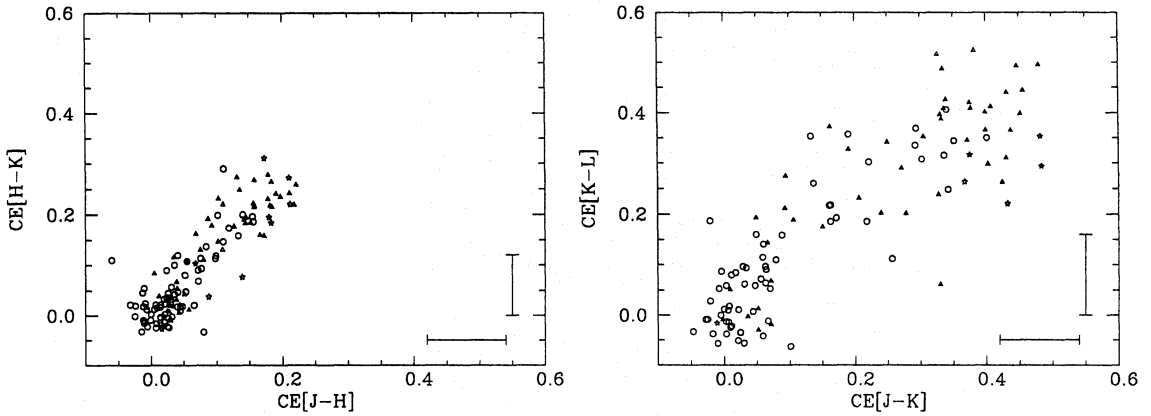

Fig. 5. Near-IR excess colour-colour diagrams for Be stars. The symbols represent different ranges of $E[B - V]$, as in Figs. 1 and 2. Typical 2σ uncertainties are shown in the lower right-hand corner

3.4. IR excess as a function of stellar parameters

As noted in Sect. 3.2 the largest colour excesses occur for stars of earlier spectral type. This is demonstrated in Fig. 4a, where the $CE[V - L]$ colour is shown as a function of spectral type, with luminosity class indicated by different symbols. For a particular spectral type there is a large scatter in the colour excess, with no apparent dependence on luminosity class. However, there is a reasonably well defined upper limit to the colour excesses that increases from late to early types, indicating that Be stars of any spectral type do not have an arbitrarily large excess. Most of the late-type stars in the sample show little or no detectable near-IR excess, even at L band (see Fig. 1). Coté & Waters (1987) observed the same phenomena in *IRAS* far-IR excess colours.

It is likely that stellar rotation plays a role in the formation of a Be star from a B star since Be stars, on average, have large projected rotational velocities compared to normal B-type stars. Struve (1931) suggested that the formation of the circumstellar envelopes around Be stars is due to ejection of material induced by rapid rotation. If this is the case, then a correlation between excess and rotational velocity is expected. In Fig. 4b the excess at L band is shown as a function of $v \sin i$. Values of $v \sin i$ were taken from Slettebak (1982) and the BSC. No correlation is apparent within the large scatter in the data. Also note that the stars with little or no excess have a similar distribution of $v \sin i$ as the stars with large excess. Gehrz et al. (1974) and Coté & Waters (1987) also found no apparent correlation between $v \sin i$ and near-IR and far-IR excess respectively. There is a small number of stars with large colour excess that have a lower $v \sin i$ than the majority of stars in the survey. This may be accounted for by the influence of the inclination angle. If the programme stars have a uniform distribution of inclination angles, a small number of stars will have low values of $v \sin i$. Clearly, a connection between rotational velocity and the near-IR excess of Be stars is not evident from our observations. In a study of the far-IR excess of both B and Be stars, Waters (1986a) concludes that rotation facilitates the presence of circumstellar material but additional mechanism(s) determine whether or not a B star becomes a Be star.

3.5. IR colour excess of Be stars

The visual–IR colour excess may be affected by the overestimation of V band brightness due to overestimation of $E[B-V]$.

The IR excess colours are derived from the expression

$$CE[m_{\lambda_1} - m_{\lambda_2}] = CE[V - m_{\lambda_2}] - CE[V - m_{\lambda_1}],$$

and are independent of V, and hence are almost independent of $E[B-V]$. In addition, these colours are free of any effects of variability at optical wavelengths. The IR colour excesses are shown in Fig. 5 as a function of two different colour combinations. If it is assumed that there is no error in the $[B-V]_o$ colour of the stars, then the uncertainty in the IR excess colours are $0\overset{m}{.}07$ for the colours incorporating the J, H and K bands and $0\overset{m}{.}08$ for those with L band. These uncertainties were derived using the uncertainties in the intrinsic colour relationships for B-type stars (Dougherty et al.1993b) and those quoted in Sect. 3.3.

The IR excess colour-colour relationships in Fig. 5 show a similar behaviour. Stars are clustered around the origin which is the base of a "banana" shaped trend that terminates at a redder colour in both axes. The stars clustered around the origin are the stars that have either little or no excess over the wavelength range of the colours under consideration, or are stars for which the circumstellar emission has the same colour as the underlying photosphere. For circumstellar material to have colours similar to the underlying photosphere requires that the circumstellar excess is constant as a function of wavelength. This seems an unlikely scenario for most of the stars at the origin since the number of stars clustered at the origin appears to decrease with longer wavelength colours, as expected for excess emission due to optically thin or partially optically thick bremsstrahlung. If the zero colour excess in Fig. 5 is due to lack of circumstellar emission at those wavelengths, and the star has any circumstellar material, then an excess of emission will appear at longer wavelengths. It may be that the excess is not apparent until the far-IR, or even longer, wavelengths.

4. IR excess from a simple disc model

In this section the effects of the structure of the circumstellar plasma distribution on the near-IR excess emission is investigated using the simple disc model of Waters (1986b).

4.1. Description of the model

The energy distribution of Be stars consists of a contribution from the photosphere of the underlying B star and a contribution from the circumstellar material that gives rise to the excess emission. If the de-reddened observed flux and the photospheric flux at frequency ν are $F_\nu^{\rm tot}$ and F_ν^* respectively, then the excess flux, F_ν^e, due to circumstellar material is

$$F_\nu^e = F_\nu^{\rm tot} - F_\nu^*. \tag{1}$$

Let us place a Be star at the origin of a Cartesian coordinate system (x', y', z') and introduce the dimensionless coordinates (x, y, z), where $x = x'/R_*$ *etc.* and R_* is the stellar radius

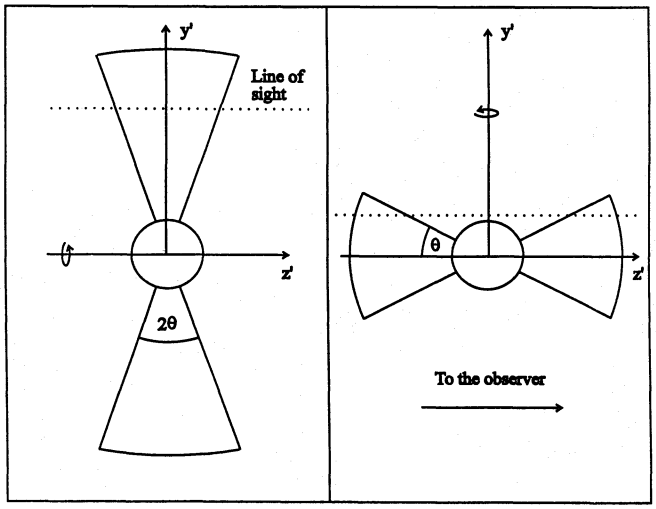

Fig. 6a and b. The $x' = 0$ cross section of the disc model of the circumstellar plasma distribution around a Be star for **a** pole-on and **b** equator-on cases. The parameters are defined in the text. The axis of rotation is indicated for the two cases

(Fig. 6). For isothermal plasma of temperature T_d the excess flux at frequency ν is given by

$$F_\nu^e = \int_{\Omega \neq \Omega_*} B_\nu(T_d)(1 - e^{-\tau_\nu(x,y)})\, d\Omega + \int_{\Omega=\Omega_*} [B_\nu(T_d) - I_\nu^*](1 - e^{-\tau_\nu(x,y)})\, d\Omega, \tag{2}$$

where Ω_* is the solid angle subtended by the stellar photosphere, $B_\nu(T_d)$ is the Planck function for temperature T_d, I_ν^* is the intensity of the photospheric emission, and $\tau_\nu(x, y)$ is the optical depth along the line of sight defined by (x, y). The first integral represents the contribution to the flux from the plasma along lines of sight that do not intersect the stellar disc, and the second integral the flux from lines of sight that intersect the stellar disc.

The IR emission from the circumstellar envelopes of Be stars arises from free-free and bound-free processes. For a radially symmetric disc of isothermal plasma with opening angle θ and a radial density distribution of the form

$$\rho(r) = \rho_o \left(\frac{r}{R_*}\right)^{-\beta} \tag{3}$$

that extends to a radius R_d, where ρ_o is the density of the circumstellar plasma at $r = R_*$, it can be shown that the optical depth is given by an equation of the form

$$\tau_\nu(x, y) = aC(\nu, T_d)\rho_o^2 R_* \int_\zeta^\xi (x^2 + y^2 + z^2)^{-\beta}\, dz, \tag{4}$$

where a is a constant equal to 1 or 2, ξ and ζ are upper and lower limits of integration and

$$C(\nu, T_d) = 3.692 \times 10^8 (1 - e^{-h\nu/kT_d})(Z/\mu m_H)^2 T_d^{-\frac{1}{2}} \nu^{-3} \gamma \{g_{\rm ff}(\nu, T_d) + g_{\rm bf}(\nu, T_d)\}, \tag{5}$$

where Z is the mean atomic charge, γ is the ratio of electrons to ions, μm_H is the mean atomic weight of the ions, and $g_{\rm ff}$ and $g_{\rm bf}$ are the Gaunt factors for free-free and bound-free emission at frequency ν and temperature T_d.

4.2. Theoretical magnitudes

To obtain magnitudes from the theoretical excess flux F_ν^e at each passband of interest, the Geneva passbands (Rufener & Nicolet 1988) and the *ESO* IR passbands (Bersanelli et al.1991) were convolved with the theoretical excess spectrum. The Kurucz (1979) model atmospheres for B stars were used for the intensity of the photospheric emission. The Geneva passbands were calibrated with respect to the Kurucz model atmosphere of α Lyr ($T_{\rm eff}$ = 9400K, log g = 3.95) and a V band magnitude of $0\overset{\rm m}{.}061$ (Rufener 1988). The IR passbands (m_λ) were calibrated using a blackbody of 11 200 K (Bersanelli et al. 1991) with $[V-m_\lambda]=0.0$ and normalised to an absolute flux 3.53×10^{-19} erg s^{-1} cm^{-2} μm^{-1} at 548.8 nm (Rufener & Nicolet 1988).

4.3. Parameter study

The disc model is defined in terms of the following parameters: density index β, disc radius R_d, opening angle θ, inclination angle i, radius of the underlying star R_*, and plasma temperature T_d. The effect of the different parameters on the excess colours is shown in Fig. 7. The curves represent the theoretical excess colours for increasing density ρ_o. For these relationships a stellar photosphere with $T_{\rm eff}$ = 15 000 K, log g = 4.0 and $R_*=6R_\odot$ is assumed, representing a B5 star. The effect of increasing or decreasing the photospheric temperature is to make the theoretical excess colours redder and bluer respectively. However, the change in the theoretical excess colours is small. At most, in the case of a pole-on disc around a B0 star the excess colour is $0\overset{\rm m}{.}05$ redder in both the $[J-K]$ and $[K-L]$ excess colours.

4.3.1. Effect of density index

The $[K-L]$ colour excess is shown in Fig. 7a as a function of the density of the disc at the stellar surface i.e. $\rho_o=\rho(R_*)$, for infinite pole-on discs with a range of density indices (β = 2.0 – 5.0). Also included in the diagram is the behaviour of the excess colours for edge-on infinite discs with β = 3.0 and 4.0. Features on the curve are labelled $A-C$.

At sufficiently low densities there is no excess colour since the photospheric emission dominates the total flux from the star–disc system. For higher densities the excess emission becomes apparent. At first the disc emission is optically thin at both K and L bands and the excess is independent of the density index (point A). This is expected for optically thin emission, since in this case the excess is proportional to the emission measure of the circumstellar plasma, which is a function of the total number of electron-ion pairs in the plasma, and not the structure of the plasma. At higher densities, L band emission becomes partially optically thick and the excess colour is now dependent on β (part B). As the density increases further the K band emission also becomes partially optically thick and the $[K-L]$ excess colour ceases to change significantly.

The value of the excess colour beyond this point is dependent on β (part C), which is accounted for in the following manner. The excess colours are determined by the slope of the excess emission. For partially optically thick emission from a radially symmetric circumstellar envelope of infinite extent with a radial density distribution of the form given in Eq. 3, the spectral index α ($F_\nu\propto\nu^\alpha$) of the excess emission spectrum is related to the density index (e.g. see Wright & Barlow 1975) by

$$\alpha=\frac{4\beta-6.2}{2\beta-1}. \tag{6}$$

Since α is a function of β for partially optically thick plasma the excess colours are also a function of β. When both the K and L band emission are partially optically thick, the slope of the excess spectrum is a constant, given by Eq. 6. The excess colour is bluer for higher density indices since the spectral index increases as β increases.

In Fig. 7b the curves of Fig. 7a are transformed to the colour-colour plane. The letters $A-C$ referring to the same points as in Fig. 7a. Since the $[K-L]$ excess colour reddens at lower densities than the $[J-K]$ excess colour, the colour-colour curve has the characteristic "banana" shape. At point C, the $[K-L]$ excess colour has reached its maximum value. However, at this value of density, the J band emission is still optically thin. For higher values of ρ_o the $[J-K]$ colour continues to redden until at sufficiently higher densities the J band emission becomes partially optically thick and the colour-colour relationship terminates (point D). The excess colour at the termination point is lower for higher values of β. Steeper excess spectra *i.e.* higher values of α, give bluer excess colour.

Also shown in Fig. 7a is the excess colour for edge-on discs with β = 3.0 and 4.0. In pole-on discs the excess colours are reddened because the total emission is the disc emission added to the stellar emission. In edge-on discs, stellar flux is attenuated, dependent on the temperature of the disc material. This is discussed in detail in Sect. 4.3.3. The size of the effect is dependent on the competition between the attenuation of stellar flux and the emission from the disc material. The excess colours are bluer for higher values of β. This is because for a given ρ_o, at higher values of β the disc material contributes less to the total flux.

4.3.2. Effect of disc radius

At a certain radius R_1, the optical depth of the circumstellar plasma is unity. This is often referred to as the "photosphere" of the circumstellar plasma and is dependent on density ρ_o and wavelength λ as

$$R_1\propto\lambda^{2.1/2\beta-1}\rho_o^{2/2\beta-1}. \tag{7}$$

If the material extends to infinity the disc is either totally optically thin i.e. $R_1\le R_*$ or partially optically thick $R_1>R_*$. However, if the material has a finite extent *i.e.* truncated at R_d,

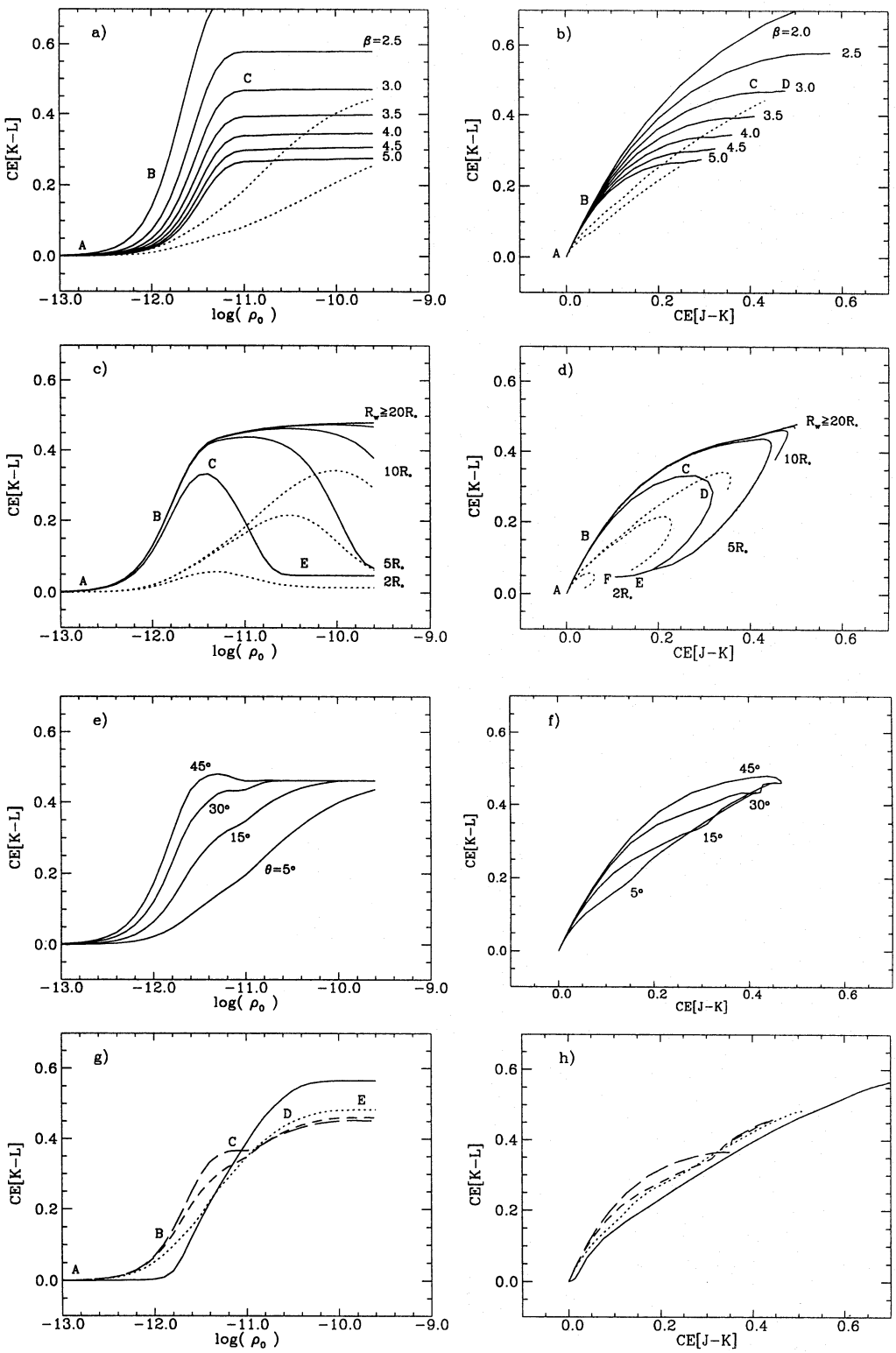

Fig. 7a–h. Effect of model disc parameters on the theoretical excess colours. In the left-hand column the $[K-L]$ colour excess is given as a function of the density of the circumstellar material at the stellar surface i.e. $\rho_o = \rho(R_*)$. The right-hand column shows the excess colour-colour relationships. The underlying photosphere was taken to be $T_{\rm eff}$ = 15 000K, log g = 4.0 and R_* = $6R_\odot$. **a** and **b** Effect of density index β with $\theta = 5^o$, $R_d = \infty$ and $T_d = 0.8T_{\rm eff}$. Solid curves are for an infinite pole-on disc with β = 2.0 − 5.0. The dashed curves are for an edge-on disc with β = 3.0 and 4.0. **c** and **d** Effect of disc radius R_d, with $\theta = 5^o$, $T_d = 0.8T_{\rm eff}$ and β = 3.0. Curves for R_d = 2, 5, 10, 50, 100R_* and ∞ for pole-on discs (solid) and edge-on discs (dashed) are shown. The curves for $R_d \geq 20R_*$ are superimposed. **e** and **f** Effect of opening angle θ on an infinite, edge-on disc with β = 3.0 and $T_d = T_{\rm eff}$. θ = 5, 15, 30 and 45°. **g** and **h** Effect of disc temperature T_d on an infinite edge-on disc with β = 2.0 and $\theta = 15^o$. T_d = 0.3 (solid), 0.7 (dotted), 1.0 (dashed), and 1.3$T_{\rm eff}$ (long dashed)

the material can be totally optically thick. The wavelength at which the emission becomes optically thick is dependent on ρ_o, β and R_d. For isothermal optically thick emission $\alpha = 2$, the slope of the Rayleigh-Jeans tail of a blackbody spectrum. Since the photospheric emission in the near-IR can be approximated by the Rayleigh-Jeans tail of a blackbody, the photosphere will also have a spectral index at near-IR wavelengths ~ 2. Therefore, the IR excess colour for optically thick near-IR circumstellar emission will be close to zero.

Figures 7c and d show the effect on excess IR colour of reducing the disc radius for discs of increasing density. For these calculations we have set $\theta = 5^o$, $\beta = 3.0$ and $T_d = 0.8T_{\rm eff}$. For sufficiently small discs, the excess colours reach a maximum value and then get bluer. This characteristic shape arises because the emission at IR wavelengths is totally optically thick i.e. $R_1 > R_d$, for values of ρ_o that are sufficiently high. At low densities the IR emission is optically thin (point A). As density increases, the L band (point B) and K band emission (point C) become partially optically thick, as in Figs. 7a and b. If the disc is sufficiently small, the near-IR emission will be optically thick. In this case, at densities higher than at point C, L band is optically thick and the excess at L is a constant function of wavelength. Since the K band emission is still partially optically thick, the excess at K continues to increase with increasing ρ_o. Hence, the excess $[K - L]$ colour begins to get bluer. When the K band emission becomes optically thick the excess colour becomes constant (point E), at a value close to zero. The totally optically thick excess colour is independent of the density index of the circumstellar material, since for optically thick plasma $\alpha = 2.0$. The dependence of the $[J - K]$ excess colour on ρ_o has the same morphology, except that the same effects occur at higher densities.

The excess colour-colour diagram for discs of different radii is shown in Fig. 7d. The letters $A - E$ refer to the corresponding points in Fig. 7c. At point D, the $[J - K]$ excess colour reaches a maximum value because the J band emission is partially optically thick. For sufficiently high density and small enough discs, the J band emission can become totally optically thick and the $[J - K]$ colour attains a constant value close to zero.

The following features are apparent in the colour-colour relationships for truncated discs. Circumstellar discs larger than $R_d \sim 20R_*$ do not have emission that becomes totally optically thick at near-IR wavelengths within the range of density ρ_o considered. For these discs the colour-colour relationships reach a terminator point as described for infinite discs in the Sect. 4.3.1. For $R_d = 10R_*$ the disc is not sufficiently small that for $\rho_o = 10^{-9.6}$ g cm^{-3} the K band emission is totally optically thick. It is evident from the relationship between the $CE[K - L]$ colour and ρ_o that for $\rho_o \sim 10^{-9.6}$ g cm^{-3} and $R_d = 5R_*$ the K band emission remains partially optically thick. For the emission at K band to be totally optically thick at this density the disc has to have a radius of less than $5R_*$. In the edge-on case, the excess colour-colour relationships have the same morphology as in the pole-on cases except that for a given density and radius the excess colour is bluer, as explained in the previous section.

4.3.3. The effect of opening angle and disc temperature

Waters (1986b) has shown that for pole-on, isothermal discs, the slope of the excess emission spectrum is independent of opening angle and the temperature of the disc plasma. In the edge-on case where there is circumstellar material along lines of sight to the underlying star, the opening angle and the temperature of the plasma affect the excess colour. For edge-on models, the $[K - L]$ colour excess is given in Fig. 7e as a function of ρ_o for opening angles of 5, 15, 30 and 45^o. Similar relationships as seen for $CE[K - L]$ can also be found in the other IR excess colours, but they occur at different values of ρ_0.

Inspection of Fig. 7e shows that the curves have very different shapes for different model parameters, but the $[K - L]$ excess colour always reaches the same asymptotic value for different values of θ. This can be understood by noting that the spectral index for partially optically thick plasma is independent of opening angle (Waters 1986b) and hence, so is the $[K - L]$ colour excess when the density is sufficiently high.

For edge-on discs, the $[K - L]$ colour excess shows some interesting effects if the temperature of the disc is varied relative to the photospheric temperature. In Fig. 7g the colour excess as a function of ρ_o for four disc temperatures (0.3, 0.7, 1.0 and 1.3 $T_{\rm eff}$) is shown. These effects can be understood by noting that the source function in the disc, the Planck function $B_\nu(T_d)$, is not equal to the stellar specific intensity. In the edge-on disc case, the circumstellar material along lines of sight that intersect the stellar surface have to be considered. The excess emission from plasma along these lines of sight is given by the second term in Eq. 2, namely

$$\int_{\Omega=\Omega_*} [B_\nu(T_d) - I_\nu^*](1 - e^{-\tau_\nu(x,y)})\, d\Omega, \qquad (8)$$

Three cases can be distinguished: where the circumstellar disc has a temperature such that $B_\nu(T_d) \ll I_\nu^*$, $B_\nu(T_d) \simeq I_\nu^*$, and $B_\nu(T_d) \gg I_\nu^*$. If the disc is much cooler than the star (e.g. $T_d = 0.3T_{\rm eff}$) the material projected against the surface of the star will absorb stellar photospheric flux, and will emit radiation with a much smaller source function. This can result in a net flux deficiency, depending on the contribution of material which is *not* projected against the star i.e. the first term in Eq. 2. In the intermediate case ($T_d \sim 0.7-1.0T_{\rm eff}$) the source function of star and disc are roughly equal, and no net effect is expected from the absorption of stellar flux, since it is replaced by disc emission with comparable source function. For high temperature discs there is net emission from the material along lines of sight that intersect the stellar disc. This is because the source function in the disc is higher than that of the stellar intensity. In this case, when lines of sight towards the star become partially optically thick at L band, the $[K - L]$ colour excess will redden (B). When density is increased, a circumstellar emission along lines of sight to the star will be partially optically thick at K band and the $[K - L]$ colour excess will be constant (C). This is the same effect as described in Figs. 7a and b. However, in the case of an edge-on disc as density is increased further, lines of sight that do *not* intersect the stellar disc will become partially optically

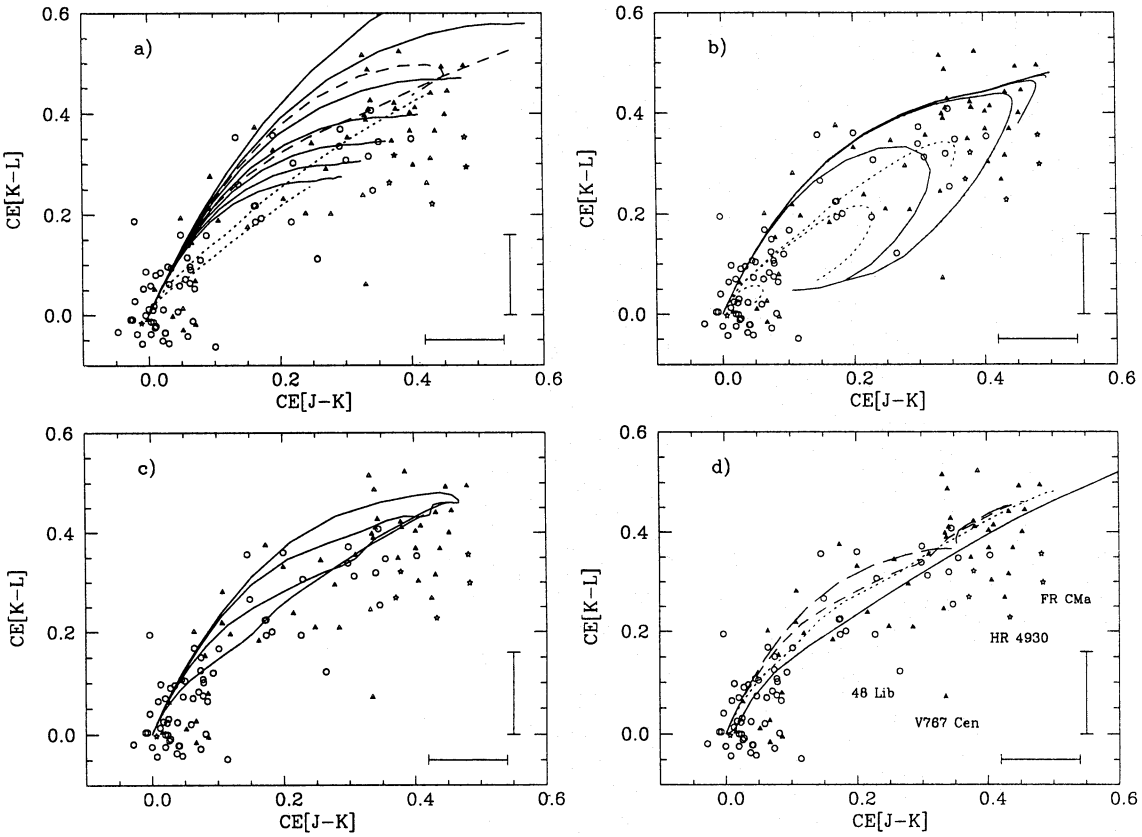

Fig. 8a–d. Theoretical $[K-L], [J-K]$ excess colour-colour relationship applied to the observed IR excess colour relationships of Be stars. The curves represent the theoretical relationships for the different values of β, R_d, θ and T_d for both pole-on and edge-on discs given in Fig. 7b, d, f, and h. See Fig. 7 for model parameters. Typical 2σ uncertainties are shown in the lower right-hand corner of each diagram

thick, first at L band (D) and then at K band (E). This will result in a further increase (D) of the excess colour to another constant value (E).

Combining the colour excess of two IR colours in a colour-colour diagram, the model tracks show the behaviour as shown in Fig. 7h. The models reach different asymptotic points in the colour-colour diagram for different disc temperatures. This is due to the fact that the source function is different. In particular, the slope of the Planck function in the near-IR is significantly different for the 5000, 10 000 and 15 000 K models.

4.4. Comparison of theoretical and observed excess colours

In Fig. 8, the theoretical excess colour-colour relationships are compared to the observed colours. It is clearly seen that a large number of stars have near-IR excess emission that is partially optically thick. Thus, in principle, it is possible to determine the structure of the circumstellar plasma around many Be stars up to a radii of a few R_* from the near-IR excess emission.

Given the uncertainties in the excess colours, the effects of disc opening angle, inclination angle and temperature are not sufficiently large that they can be discerned from the near-IR excess alone, though the lack of excess larger than $\sim 0\overset{m}{.}5$ in both axes argues against high density ($\rho_o \gtrsim 10^{-11}$ g cm^{-3}) discs as cool as 5000 K (Fig. 8d). Throughout the remainder of the paper an opening angle of 5^o and a disc temperature of 12,000 K are adopted.

The parameters that have the most significant effect on the position in the excess colour-colour diagram are the density of the plasma ρ_o, the density index β and the radius of the disc R_d. It is clearly seen that varying the density produces the same characteristic banana shape as seen in the observations, *independent* of the model parameters. This indicates that the factor responsible for producing the general trend observed in the excess colour-colour relationships is a large range in the density of the circumstellar material, up to $\rho_o \sim 10^{-9.5}$ g cm^{-3}. The excess colours in Fig. 8a and b are consistent with with discs of plasma of radius greater than $5-10R_*$, and density index $\sim 2.0-5.0$. The upper limit to the density index is difficult to discern. For pole-on discs a few stars require density indices ~ 5.0 or higher ,or $R_d \leq 2R_*$. With edge-on discs the excess colours of these stars can be satisfied with density indices $\sim 3.0-4.0$ and large discs. The range of density index is in good agreement with $2.0 < \beta < 3.5$ for Be stars determined by Waters et al. (1987) from *IRAS* far-IR observations.

A number of excess colours cannot be reconciled by a disc with a single density index extending to large radii. These lie to the left and below the loci of curves in Figs. 8a, c and d. The most extreme examples are FR CMa, HR 4930, V767 Cen, and

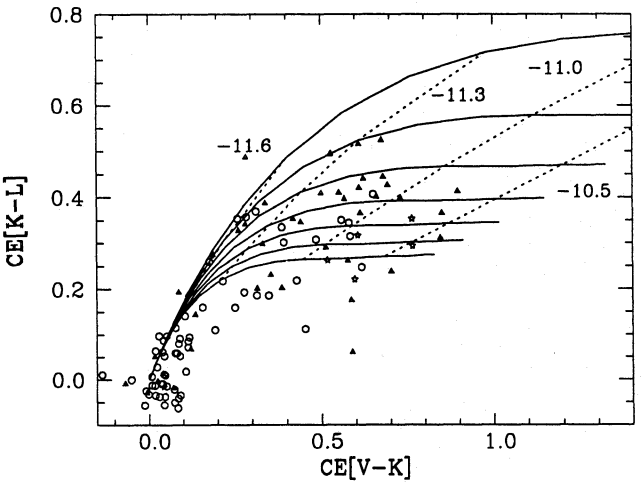

Fig. 9. The excess $[K - L]$ colour as a function of $[V - K]$ excess colour. The solid lines are the theoretical relationships for $\beta = 2.0, 2.5, 3.0, 3.5, 4.0, 4.5$ and 5.0 for pole-on discs. Other model parameters are as in Fig. 7a. The dashed lines denote different values of $\log \rho_o$

48 Lib. These stars can be better fit by discs with optically thick turnovers at near-IR wavelengths. This corresponds to small discs i.e. $R_d \sim 2 - 5R_*$. However, stars with discs of radii $2 - 5R_*$ should have smaller colour excess at wavelengths longward of the near-IR, since they are totally optically thick at these wavelengths. The stars FR CMa, HR 4930 and 48 Lib each had an excess at far-IR wavelengths at the epoch of the *IRAS* observations (Waters et al.1987). At first glance, this may seem to pose a problem for the interpretation of the near-IR excess colours as arising from truncated discs. However, both these stars has a history of variations in both visual and IR continuum and in Hα line emission (e.g. Slettebak 1982; Dougherty & Taylor 1994). It is reasonable to suggest that these stars may not have had a large excess at far-IR wavelengths at the epoch of the near-IR and visual observations discussed here.

As mentioned, the position of a star in the IR excess colour-colour diagram is strongly dependent on the density. The density is best constrained by examining the excess emission at a particular wavelength. In Fig. 9 the excess $[K - L]$ colour is shown as a function of excess $[V - K]$ colour. If it is assumed that the V band emission is photospheric then $CE[V - K]$ represents the excess emission at K band. From the figure, it is seen that the density ρ_o of the circumstellar plasma is less than 10^{-11} g cm^{-3} for most of the sample stars. A few stars appear to have values of ρ_o as high as $10^{-10.5}$ g cm^{-3}. If truncated discs apply to these few stars then the density can be lower i.e. $\sim 10^{-11}$ g cm^{-3}. For edge-on discs, assuming the same opening angle as the pole-on discs, the deduced densities will be a little higher. For the IR excess to be detectable i.e. $CE[K - L] \gtrsim 0\overset{m}{.}24$, $CE[V - K] \gtrsim 0\overset{m}{.}21$, the density has to be at least $\sim 10^{-11.6}$ g cm^{-3} for $\beta \sim 2.0$. This range of densities for the circumstellar plasma is in good agreement with those found by Waters et al. (1987) from analysis of *IRAS* far-IR observations of 69 Be stars.

5. Discussion

For the bulk of the sample stars, the near-IR excesses can be fit with disc models that are consistent with model fits to the excess at far-IR wavelengths, namely discs of radii greater than $\sim 10R_*$ and with a single density index in the range $2.0 - 5.0$. It is not possible from near-IR colours alone to discern the effects of opening angle and disc temperature. A small number of Be stars appear to have discs that are truncated at small radii. Small discs have been noted before. Coté & Waters (1987) conclude from analysis of far-IR observations of η Centauri that it has a small circumstellar disc. The range of sizes of the truncated discs determined in this study is similar to the sizes inferred from Hα line profiles by Dachs et al. (1986). However, the Hα line profiles were interpreted as arising from circumstellar plasma in a gravitationally bound disc of finite radius $\sim 2 - 10R_*$. There is substantial evidence that the high density discs around Be stars contain material that has a substantial radial velocity. This material extends to large distances from the underlying star, and may escape. The X-ray luminosity in Be/X-ray binaries suggests that the neutron star is embedded in a high density plasma with outflow velocities of the order of 100 to a few 100 km s^{-1} at the orbital distance of the neutron star, typically 10 to $100R_*$ (Waters et al.1988b). Observations of Be-shell stars in the far-UV reveal blue asymmetries in lines of low ionisation e.g. Fe III, that originate in the high density plasma, with velocities up to 150 km s^{-1}. Though the radius at which these lines are formed in the plasma is uncertain, they indicate that high radial velocities are attained by the plasma (Oegerle & Polidan 1984). Radio observations of six Be stars require that the circumstellar material extends to very large distances from the underlying star, from several hundred $R_\odot$ (Taylor et al. 1990) up to $\sim 2000R_\odot$ in the case of ψ Per. If material with high radial velocity extends to such large radii, then the escape velocity can be exceeded and the material escape (Dougherty & Taylor 1992).

From the above discussion, it appears unlikely that discs of small radius exist around Be stars. If this is the case, how are the excess IR colours of these stars explained in a manner consistent with observations at longer wavelengths? Continuum observations at far-IR, millimeter and radio wavelengths indicate that there is a structure change in the circumstellar plasma at large radii in 21 Be stars that have been observed at radio wavelengths. This structure change is evident by a turndown in the far-IR/millimeter region of the spectrum (Taylor et al.1987; Waters et al.1991). The density indices inferred from the far-IR observations are $\sim 2.5 - 3.0$ (Waters et al.1987) whereas the radio spectral indices suggest $\beta \sim 4.0$ (Dougherty et al.1991b).

If such a change in density index were to occur at sufficiently small radius, then the turndown may occur in the near-IR part of the spectrum. In the case of a truncated disc, the density index goes from some finite value to infinity at the outer edge of the disc. This gives rise to an optically thick turndown to $\alpha = 2$ in the excess emission spectrum. If the density index changes from one finite value to another at some radius, the spectrum will turn over, but not to that of totally optically thick emission.

The presence of turndowns at different wavelength regimes in the continuum spectra of Be stars makes it tempting to speculate that the turndowns are all due to the same underlying physical mechanism, which is evident at different radii in different Be stars. At this time it is not clear what physical mechanism(s) could cause such a feature in the spectrum. Taylor et al. (1990) proposed several mechanisms, including recombination and acceleration of the plasma at large radii. Recombination of ions in the plasma would give rise to the number density of ions decreasing more rapidly with radius. In this case one would expect there to be a correlation between UV photon luminosity (or spectral type) and the change in the spectral index across the turndown. However, such a correlation is not apparent in the radio detected Be stars. Waters et al. (1991) suggest that the UV photon flux from the polar regions of the underlying star accelerates the plasma via radiation pressure. In this scenario, the radius at which the radiation pressure takes effect is determined by the UV photon flux and the column density of the plasma as a function of radius, which in turn is a function of both the density index of the plasma and the plasma density at the base of the circumstellar disc. Where the column density is too high the UV photons are effectively blocked from the plasma. At the radius where the density of the plasma is sufficiently low, the photons can penetrate into the disc and accelerate the wind.

6. Summary

In this paper we have presented quasi-simultaneous observations of a large sample of Be stars at near-IR and visual wavelengths in order to derive colour excesses that are independent of temporal variations. Colour-colour diagrams were used to examine the nature of the excess emission. It was found that the excess increases with wavelength, as expected for excess emission arising from free-free and bound-free processes. The largest colour excess occurs for early spectral types. The IR colours of 51 Oph, AX Mon, HR 2577 and HR 2545 were found to be markedly different to the remainder of the sample. In the case of 51 Oph, the circumstellar emission is attributed to dust. The emission from the other three stars is due to the presence of a late-type companion star. The colours of β Mon and CX Dra also suggest the presence of a companion star of spectral type A or F.

The near-IR excess colours were calculated for the sample stars. The fraction of stars with colour excess increases with wavelength, with $\sim$ 500% and 60% of the stars having a significant colour excess at K and L pass bands. No correlation between colour excess and $v \sin i$ was apparent. The near-IR excess colour-colour relationships of Be stars have a "banana" shaped trend that originates at zero colour excess and extends to redder colour values. This morphology is attributed to circumstellar envelopes of different density.

Theoretical near-IR excess colours were derived for emission from a simple disc model with a radial density distribution of the form $\rho \propto r^{-\beta}$. The strong dependence of the colour-colour relationships on density ρ_o, density index β and the radius of the disc was demonstrated.

The excess IR colours of many Be stars indicate that the near-IR emission is partially optically thick. The near-IR excess emission from the majority of Be stars can be reconciled by a circumstellar disc of plasma with a density index in the range $2.0 - 5.0$ out to radii greater than $\sim 10R_*$. The largest colour excess detected requires a density $\rho_o \sim 10^{-10.5}$ g cm^{-3}. For the near-IR colour excess to be detectable at K and L band, ρ_o has to be greater than $\sim 10^{-11.6}$ g cm^{-3}. Both the density index range and the density ρ_o determined here are in good agreement with those found by Waters et al. (1987) based on *IRAS* far-IR data.

The colour excess of a number of stars require that either the circumstellar disc is truncated or the density index changes at a few stellar radii from the underlying star. In at least one Be star, ψ Persei, disc truncation at such small radii is inconsistent with observations at longer wavelengths. From far-IR, millimeter and radio observations, turndowns in the spectra of Be stars are apparent at wavelengths that differ strongly from star to star. It is speculated that these turndowns may be the result of the same physical mechanism operating at different radii within the circumstellar plasma.

Acknowledgements. SMD acknowledges the hospitality and financial support of the SRON Laboratory for Space Research, Groningen during his stay in Groningen. SMD was also supported by an Izaak Walton Killam Memorial Scholarship. This research was also supported by a grant to ART from the National Sciences and Engineering Research Council of Canada. The research of LBFMW was financially supported by a grant from the Royal Dutch Academy of Arts and Sciences.

References

Allen, D.A. 1973, MNRAS, **161**, 145
Beeckmans, F., Hubert-Delplace, A.M. 1980, A&A, **86**, 72
Bersanelli, M., Bouchet, P. Falomo, R. 1991, A&A, **252**, 854
Coté, J., Waters, L.B.F.M. 1987, A&A, **176**, 93
Cramer, N. 1982, A&A, **112**, 330
Cramer, N. 1984, A&A, **132**, 283
Cramer, N., Maeder, A. 1979, **78**, 305
Dachs, J., Engels, D., Kiehling, R. 1988, A&A, **194**, 167
Dachs, J., Hanuschik, R., Kaiser, D., Ballereau, D., Bouchet, P., Kiehling, R., Kozok, J., Rudolph, R., Schlosser, W. 1986, A&AS, **63**, 87
Dougherty, S.M., 1993a, PhD., University of Calgary
Dougherty, S.M., Cramer, N., van Kerkwijk, M.H., Taylor, A.R., Waters, L.B.F.M. 1993b, A&A, **273**, 503
Dougherty, S.M., Taylor, A.R. 1992, Nature, **359**, 808
Dougherty, S.M., Taylor, A.R. 1994, MNRAS, in press
Dougherty, S.M., Taylor, A.R., Clark, T.A. 1991a, AJ, **102**, 1753
Dougherty, S.M., Taylor, A.R., Waters, L.B.F.M. 1991b, A&A, **248**, 175
Gehrz, R.D., Hackwell, J.A., Jones, T.W. 1974, ApJ, **191**, 675
Goraya, P.S. 1984, A&A, **138** 19
Hoffleit, D., Jaschek, C. 1982, *The Bright Star Catalogue*, Yale University Observatory, New Haven, USA
Hoffleit, D., Saladyan, M., Wlasuk, P. 1983, *The Bright Star Catalogue Supplement*, Yale University Observatory, New Haven, USA

IRAS Explanatory Supplement to the Point Source Catalogue, 1985, (eds. C.A. Beichman, G. Neugebauer, H.J. Habing, P.E. Clegg & T.J. Chester) JPL D-1855
Johnson, H.L. 1967, ApJL, **150**, L19
Johnson, H.L., Mitchell, R.I, Iriate, B., Wisniewski, W.Z. 1966, *Comm. Lunar Planet. Lab*, **4**, 99
Koornneef, J. 1983a, A&AS, **51**, 489
Kurucz, R.L. 1979, ApJS, **40**, 1
McLean, I.S., Brown, J.D. 1978, A&A, **69**, 291
North, P., Nicolet, B. 1990, A&A, **228**, 78
Oegerle, W.R., Polidan, R.S. 1984, ApJ, **285**, 648
Olnon, F.M. 1975, A&A, **39**, 217
Poeckert, R., Bastien, P., Landstreet, J.D. 1979. AJ, **84**, 812
Poeckert, R., Marlborough, J.M. 1976, ApJ, **206**, 182
Rufener, F. 1988, *Catalogue of stars measured in the Geneva Observatory photometric system*, 4th edn., Observatoire de Genève
Rufener, F., Nicolet, B. 1988, A&A, **206**, 357
Schild, R. 1978, ApJS, **37**, 77
Schild, R. 1983, A&A, **120**, 223
Slettebak, A. 1982, ApJS, **50**, 55
Snow, T.P. 1975, ApJ, **198**, 366
Struve, O. 1931, ApJ, **73**, 94
Taylor, A.R., Waters, L.B.F.M., Lamers, H.G.L.M., Persi, P. & Bjorkman, K.S. 1987, MNRAS, **288**, 811
Taylor, A.R., Waters, L.B.F.M., Bjorkman, K.S., Dougherty, S.M. 1990, A&A, **231**, 453
Waters, L.B.F.M. 1986a, A&A, **159**, L1
Waters, L.B.F.M. 1986b, A&A, **162**, 121
Waters, L.B.F.M., Boland, W., Taylor, A.R., van de Stadt, H., Lamers, H.J.G.L.M. 1989, A&A, **213**, L19
Waters, L.B.F.M., Coté, J., Geballe, T.R. 1988a, A&A, **203**, 348
Waters, L.B.F.M., Coté, J., Lamers, H.J.G.L.M. 1987, A&A, **185**, 206
Waters, L.B.F.M., Taylor, A.R., van de Heuvel, E.P.J., Habets, G.M.H.J., Persei, P. 1988b, A&A, **198**, 200
Waters, L.B.F.M., van der Veen, W.E.C.J., Taylor, A.R., Marlborough, J.M., Dougherty, S.M. 1991, A&A, **244**, 120
Woolf, N.J., Stein, W.A., Strittmatter, P.A. 1970, A&A, **9**, 252
Wright, A.E., Barlow, M.J. 1975, MNRAS, **178**, 41

This article was processed by the author using Springer-Verlag LaTeX A&A style file version 3.